Multi-resolution DT-MRI cardiac tractography

Ferran Poveda[1], Debora Gil[1 2], and Enric Martí-Godia[1]

[1] Computer Science Department, Universitat Autònoma de Barcelona, Spain
ferran.poveda,enric.marti@uab.es
[2] Computer Vision Center, Universitat Autònoma de Barcelona, Spain
debora@cvc.uab.es

Abstract. Even using objective measures from DT-MRI no consensus about myocardial architecture has been achieved so far. Streamlining provides good reconstructions at low level of detail, but falls short to give global abstract interpretations. In this paper, we present a multi-resolution methodology that is able to produce simplified representations of cardiac architecture. Our approach produces a reduced set of tracts that are representative of the main geometric features of myocardial anatomical structure. Experiments show that fiber geometry is preserved along reductions, which validates the simplified model for interpretation of cardiac architecture.

1 Introduction

The myocardium presents a distinctly complex architecture compared to the rest of voluntary muscles. There is an ongoing controversy on how this architecture translates into a generic geometric model and its correlation between this form and the function of the cardiac muscle. However, it is widely accepted that myocardial muscular architecture plays a critical role in key functional aspects as electrical propagation and force production. Researchers have proposed several interpretations of different conceptual models of cardiac architecture [1, 2] from either dissection or histology procedures. Still, many researchers reject these conceptual models due to the inherent complexity and subjectivity of the procedures used [3, 4]. Indeed, some recent works disagree in their architectural interpretation of the heart [2, 5]; the argument is nowhere near to a settlement.

Computer analysis of Diffusion Weighted Magnetic Resonance Imaging (DW-MRI) is the preferred approach for an objective representation of cardiac architecture. Among DW-MRI techniques, Diffusion Tensor MRI (DT-MRI) has been established as the reference imaging modality for the rapid measurement of the whole cardiac architecture. This technique provides objective discrete measurement of the spatial arrangement of myocytes by observing local anisotropic water diffusion of water molecules [6]. Due to the high level of detail of these modalities, extraction of the global architecture of the heart is not feasible by visual analysis. Currently, most research focuses on the reconstruction and representation of this

data through tractography [7–11]. This technique represents spatial coherence of the tensors information through mathematical integration of the curves defined by DT-MRI primary eigenvector. These fully detailed tractographic reconstructions have proved their validity for low-level descriptions, but might fail on a higher level of analysis because of their inherent complexity. As a consequence, interpretation may still be biased.

In this paper we introduce a multi-resolution tractography-based methodology for a comprehensive description of the myocardial fiber architecture. We use pyramidal decomposition to represent fiber spatial disposition at several levels of detail. Each reduction level takes into account fiber orientation in order to better preserve anatomical features across decreasing resolutions. Our experiments show that fiber geometry is preserved along reductions, which validates the simplified model for interpretation of cardiac architecture.

2 Multi-resolution tractography

Heart tractography [8] reconstructs cardiac muscular fibers composed by several streamlines (or fiber tracks) associated to DTI primary eigenvector. A streamline is a curve tangential to the vector field at any point of such curve. These curves cannot be solved analytically. For this reason, we reconstruct fibers using a fifth order Runge-Kutta-Fehlbert integration method with adaptive integration steps based on an estimation of the integration error. Unlike other methods, our tractographies ensure data completeness in the sense that the basal loop and the apex are reconstructed [12].

In any context, it is difficult, or even impossible, to understand the gross geometric features just by examining object details at a small scale. If we step away from the object we can get a more contextual view, providing us the opportunity to understand higher-level architectures. Computationally, this can translate in a multi-resolution approach. Multi-resolution strategies have been widely applied to process gross detail of data [13, 14], but their potential for getting abstract representations has been never used. We propose to build a multi-resolution tractography based on the reconstruction of multi-scale data.

The standard multi-scale generation approach is the linear Gaussian pyramidal representation. This technique applies a Gaussian filtering and later linear reduction via regular subsampling of the full-scale input. Reduced representations summarize the original information and represent it at different levels of detail. The reductions are statistically complete in such a way that the Gaussian smoothing keeps local information before applying subsampling.

A main concern of Gaussian approaches is that information is equally processed for any dimensions. Nevertheless, in a DT-MRI application we have structural information that can be taken as a reference for anisotropic filtering. For this reason, we argue that more robust filtering approaches should consider the anatomical directions of the muscle.

We propose using a Structure Preserving Diffusion (SPD) operator [15] oriented along DT-MRI primary eigenvector, ξ_1. Given the original volume to be

filtered, $Vol(x, y, z)$, the diffusion process is given by the following heat diffusion equation in divergence form:

$$SPD_t = \text{div}(J \nabla SPD) \quad \text{with} \quad SPD(x, y, z, 0) = Vol(x, y, z) \tag{1}$$

for ∇ denoting the gradient direction of the divergence operator, and J a symmetric tensor driving the diffusion process. In order to restrict diffusion to ξ_1, J is defined as:

$$J = Q \Lambda Q^t = \begin{pmatrix} \xi_1^1 & \xi_1^2 & \xi_1^3 \\ \xi_2^1 & \xi_2^2 & \xi_2^3 \\ \xi_3^1 & \xi_3^2 & \xi_3^3 \end{pmatrix} \begin{pmatrix} 1 & 0 & 0 \\ 0 & 0 & 0 \\ 0 & 0 & 0 \end{pmatrix} \begin{pmatrix} \xi_1^1 & \xi_2^1 & \xi_3^1 \\ \xi_1^2 & \xi_2^2 & \xi_3^2 \\ \xi_1^3 & \xi_2^3 & \xi_3^3 \end{pmatrix} \tag{2}$$

for ξ_i DT-MRI eigenvectors. In our case, (1) is applied to each of ξ_1 components. In [15] it is shown that (1) has a unique solution that corresponds to solving the heat equation along the integral curves of ξ_1.

Decimation is obtained as in the Gaussian aproach, by the posterior linear reduction via regular subsampling of the full-scale input.

2.1 Implementation details

The volume diffusion defined by equation (1) is implemented using 1-dimensional Gaussian kernels for weighting the values of the volume Vol along the direction given by ξ_1. We observe that this would imply integrating the field ξ_1 for large times (scales). In order to avoid such integration, we will iterate the basic diffusion operator given by the volume diffused a minimal time unit t_0 (scale) as seen in Fig. 1. By uniqueness of solutions to parabolic PDE [16], the k-th iteration corresponds to the solution to (1) at time kt_0. For each voxel, (x, y, z), the volume diffused at the minimal scale, $SPD(x, y, z, t_0)$, is given by:

$$\begin{aligned} SPD(x, y, z, t_0) = {} & g_{-1} SPD(x - \xi_1^x, y - \xi_1^y, z - \xi_1^z, 0) + g_0 SPD(x, y, z, 0) \\ & + g_1 SPD(x + \xi_1^x, y + \xi_1^y, z + \xi_1^z, 0) \end{aligned} \tag{3}$$

for $(g_j)_{j=-1}^1$ the coefficients of a 1-dimensional gaussian kernel of size 3. By iterating (3) k times:

$$\begin{aligned} SPD(x, y, z, kt_0) = {} & g_{-1} SPD(x - \xi_1^x, y - \xi_1^y, z - \xi_1^z, (k-1)t_0) \\ & + g_0 SPD(x, y, z, (k-1)t_0) \\ & + g_1 SPD(x + \xi_1^x, y + \xi_1^y, z + \xi_1^z, (k-1)t_0) \end{aligned} \tag{4}$$

we compute the solution to (1) at time kt_0. In the case of DTI primary eigenvector, the iteration (4) is applied to each of its components.

As in any diffusion process, boundary values deserve special treatment. In our case, due to DTI acquisition, the most undesired artifacts could appear at myocardial boundaries as a consequence of blending anatomical information with arbitrary adjacent data. A common way of coping with boundary artifacts is by propagating the values of the diffused function outside their domain of

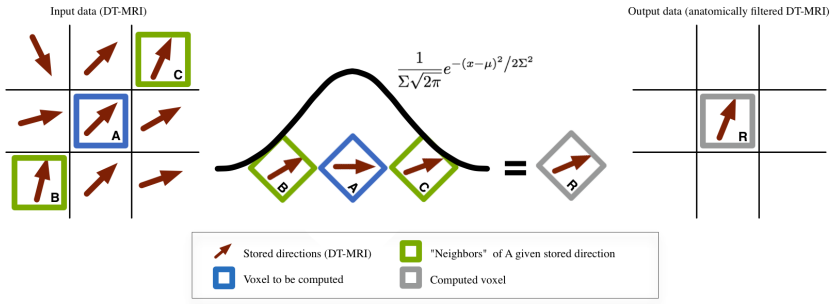

Fig. 1. Schematic example of anatomical filtering procedure

definition, that is, the myocardium. This propagation has to be performed across the domain boundaries in order to produce consistent extensions. We propose a boundary propagation based on the gradient of the distance map to a mask of the myocardial volume. Each non-anatomic voxel value is replaced by the closest boundary voxel value in the direction of the gradient.

3 Results

There are two potential sources of error in a multi-resolution tractography. Losing anatomical information in the filtering step, and errors in the tractography integration introduced by the decimation of the resolution.

The loss of information in the filtering step strongly depends on the capability of the diffusion for preserving anatomical structures. In this context, SPD is more suitable than Gaussian reductions, at least for intensity volumes. Concerning errors in the tractography integration, they are a consequence from working in the discrete domain. The tractographic integration operates on a continuous vector field extrapolated from the original discrete domain, by linear interpolation. Therefore, the impact of such interpolation on reduced scale level should be determined.

In order to asses the above sources of error, we have applied our methodology to seven ex-vivo healthy canine studies from the JHU public database [17]. The data set was arranged in about 256 x 256 x 108 array (depending on the scanned heart) where each voxel in the array consisted of 3 eigenvalues and 3 eigenvectors. Two experiments have been performed:

- **Impact of Volume filtering**: The original primary eigenvector has been compared to its filtered version using Gaussian kernels and SPD. This experiment validates which filtering is better suited for the full-scale tractography.
- **Impact of interpolation in reduced tractography**: The reduced volumes (previously filtered) have been up scaled using linear interpolation and compared to the filtered full scale volumes. This experiment allows us to

compare our simplified tractographic reconstruction performance in front of the reconstruction on original data.

In order to compare vectors we have computed voxel-wise angular differences as reported in the literature [18, 19]. Results are statistically summarized using histograms for each canine study, as well as, the central quartile of the distribution.

3.1 Impact of volume filtering

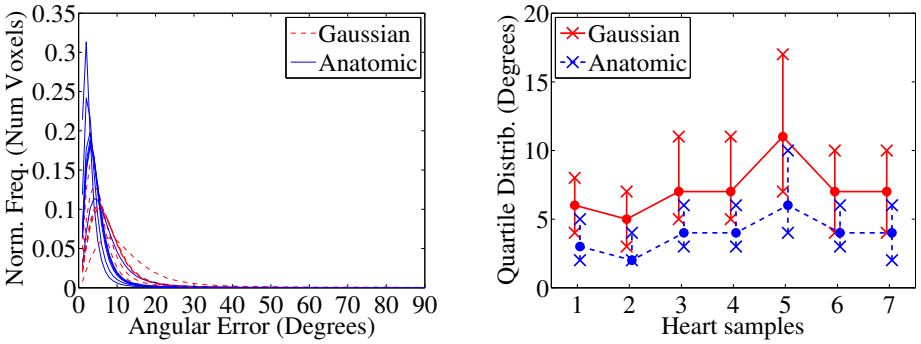

(a) Histogram traces of angular error

(b) Quartiles of angular error

Fig. 2. Voxel-wise statistics between original and filtered volumes

Figure 2 shows the histograms for Gaussian and SPD (Anatomic) filtering applied to all the canine samples, and the ranks given by the central, second and third quartiles of the distribution. First, we observe in Fig. 2(a) that the SPD histograms are the most stable ones. This is probably due to a better contextualization of myocardial anatomy. Gaussian filtering histograms significantly vary across canine anatomies. Additionally, ranges in Fig. 2(b) show that our anatomical filter performs better, having its central quartile ranging from 2 to 6 degrees. In contrast, Gaussian has considerably higher values, second quartile ranges from 5 to 11 degrees. This selects SPD as the best filtering for full-scale representations.

3.2 Impact of interpolation in reduced tractography

Figure 3 show the same description as Fig. 2 but applied to the comparison of filtered with sub-sampled volumes. Gaussian pyramidal representation its still offering an inferior performance than the SPD approach. However, in the histogram traces shown in Fig. 3(a) it is difficult to appreciate any significant difference between the two methodologies. Figure 3(b) reveals more precise differences

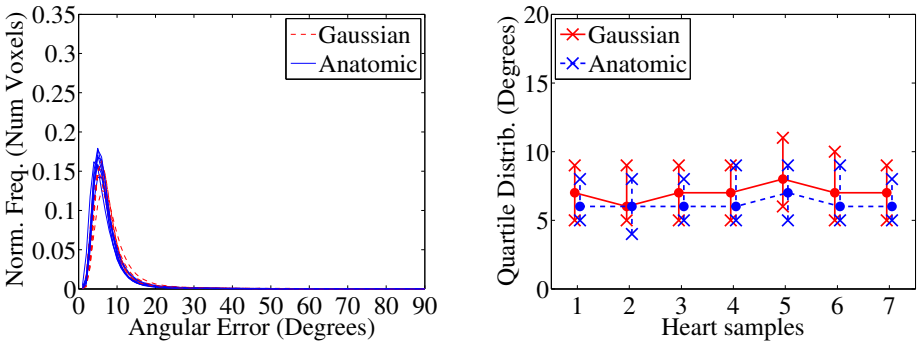

(a) Histogram traces of angular error

(b) Quartiles of angular error

Fig. 3. Voxel-wise statistics between sub-sampled (filtered and sub-sampled) and filtered volumes

between the two methodologies. In this experiment, SPD have medians in the range of 6 to 7 degrees of angular error. Gaussian presents a similar behavior ranging from 6 to 8 degrees. It is clear that the linear interpolation applied on the tractography have an stronger impact in the non-isotropic methodology. The effect of sub-sampling on the Gaussian approach is clearly smaller. At this point, we attribute the loss of power of the SPD method to the isotropic nature of the re-interpolation that is used by the integration method to obtain a continuous vector field.

3.3 Cardiac architecture interpretation

The application of this work in terms of easing the interpretation of tractography can be visually assessed. Figure 4 shows our multi-resolution tractographic reconstruction of a sample canine heart, full-scale, and simplified. The simplified model keeps the main geometric features of fibers allowing an easier identification of global tendencies. It is important to notice that differences between Gaussian and SPD reductions are not easily identifiable with naked eye. However, SPD reductions are guaranteeing us more precision for future analysis.

4 Conclusions

Tractography of Diffusion Tensor MRI has enabled a new approach for an automatic and objective representation of the heart anatomy with high detail. However, the medical research to understand cardiac form and function depends on the interpretation of the essential structures of myocardial muscular architecture. These gross structures are not easily extrapolated from micro-architectural detail.

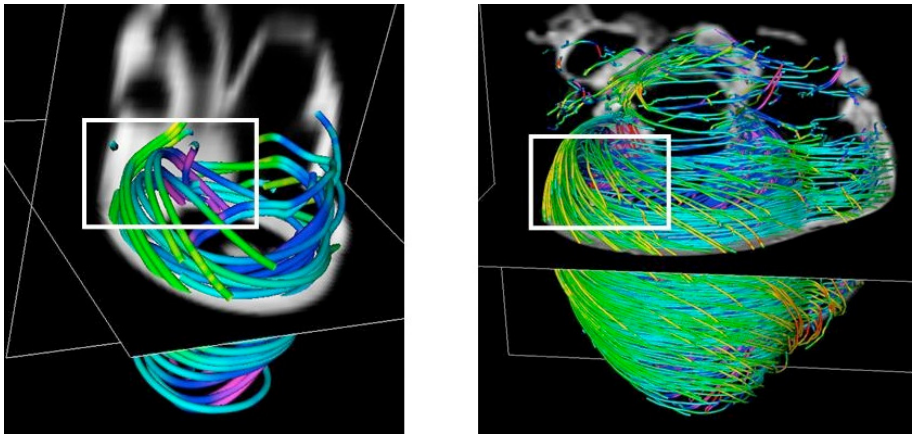

Fig. 4. Reduced (left) and full-scale (right) tractographic reconstructions of the same heart sample and a detail of the reconstruction of the complex structure of the Basal Ring.

For that reason, we have considered a multi-resolution methodology that takes into account anatomical properties from DT-MRI to represent simplified tractographies of the cardiac anatomy.

The experiments show that this physiologically informed multi-scale representation gives remarkably higher performance than the application of classical Gaussian pyramidal decompositions for the full-scale tractographic reconstruction. The volumes sub-sampled using the anatomical filtering provide slightly better results than the Gaussian approach. However, we consider that the linear isotropic nature of the bilinear interpolation used by the integration method can not take advantage of the inherent anisotropy of the anatomical filetring. Given the observed results, we are currently focusing our work on the study of the impact of multi-resolution schemes to the reconstruction. Our aim is to obtain more complete results from a geometrical study of reconstructions.

Acknowledgements

This work was supported by the Spanish projects TIN2009-13618, TIN2012-33116, and CONSOLIDER - INGENIO 2010 (CSD2007-00018). The 2nd author has been supported by The Ramon y Cajal Program. We also want to thank Drs. Patrick A. Helm and Raimond L. Winslow at the Center for Cardiovascular Bioinformatics and Modeling and Dr. Elliot McVeigh at the National Institute of Health for provision of data.

References

1. Gilbert, S.H., Benson, A.P., Li, P., Holden, A.V.: Regional localisation of left ventricular sheet structure: integration with current models of cardiac fibre, sheet

and band structure. European Journal of Cardio-thoracic Surgery **32** (2007) 231–249
2. Anderson, R., Smerup, M., Sanchez-Quintana, D., Loukas, M., Lunkernheimer, P.: The three-dimensional arrangement of the myocytes in the ventricular walls. Clinical Anatomy **22** (Jan 2009) 64–76
3. Lev, M., Simkins, C.: Architecture of the human ventricular myocardium; technic for study using a modification of the mall-maccallum method. Laboratory investigation **5**(5) (1956) 396–409
4. Grant, R.P.: Notes on the muscular architecture of the left ventricle. Circulation **32** (Aug 1965) 301–8
5. Gao, C., Lu, K., Ye, W., Li, L., Cheng, L.: Reconstruction of the architecture of ventricular myocardial fibers in ex vivo human hearts. The heart surgery forum **12**(4) (Aug 2009) E225–9
6. Scollan, D.F., Holmes, A., Winslow, R., Forder, J.: Histological validation of myocardial microstructure obtained from diffusion tensor magnetic resonance imaging. Am J Physiol **275**(6 Pt 2) (Dec 1998) H2308–18
7. Basser, P., Pajevic, S., Pierpaoli, C., Duda, J.: In vivo fiber tractography using dt-mri data. Magnetic Resonance in Medicine **44**(4) (Oct 2000) 625–632
8. Zhukov, L., Barr, A.: Heart-muscle fiber reconstruction from diffusion tensor mri. Visualization, 2003. VIS 2003. IEEE (2003) 597 – 602
9. Helm, P., Beg, M.F., Miller, M.I., Winslow, R.L.: Measuring and mapping cardiac fiber and laminar architecture using diffusion tensor mr imaging. Ann N Y Acad Sci **1047** (Jun 2005) 296–307
10. Peeters, T., Vilanova, A., Strijkerst, G., ter Haar Romeny, B.: Visualization of the fibrous structure of the heart. Vision, modelling and visualization (2006) 309–316
11. Rohmer, D., Sitek, A., Gullberg, G.: Reconstruction and visualization of fiber and laminar structure in the normal human heart from ex vivo diffusion tensor magnetic resonance imaging (dtmri) data. Investigative Radiology **42**(11) (Nov 2007) 777–789
12. Poveda, F., Gil, D., Andaluz, A., Marti, E.: Multiscale tractography for representing heart muscular architecture. In: Workshop on Computational Diffusion MRI, MICCAI. (2011)
13. Williams, L.: Pyramidal parametrics. Proceedings of SIGGRAPH **17**(3) (Jul 1983) 1–11
14. Loeckx, D., Slagmolen, P., Maes, F., Vandermeulen, D., Suetens, P.: Nonrigid image registration using conditional mutual information. IEEE Transactions on Medical Imaging **29**(1) (Jan 2010) 19–29
15. Gil, D., Hernandez-Sabate, A., Brunat, M., Jansen, S., Martínez-Vilalta, J.: Structure-preserving smoothing of biomedical images. Pat. Rec. **44(9)** (2010) 1842–1851
16. Evans, L.: Partial Differential Equations. Berkeley Math. Lect. Notes (1993)
17. Johns Hopkins University: Public dtmri dataset. `http://gforge.icm.jhu.edu/gf/project/dtmri_data_sets/` (January 2011)
18. Peyrat, J.M., Sermesant, M., Pennec, X., Delingette, H., Xu, C., McVeigh, E., Ayache, N.: A computational framework for the statistical analysis of cardiac diffusion tensors: Application to a small database of canine hearts. IEEE Transactions on Medical Imaging **26**(11) (Nov 2007) 1500
19. Lombaert, H., Peyrat, J.M., Croisille, P., Rapacchi, S., Fanton, L., Clarysse, P., Delingette, H., Ayache, N.: Statistical analysis of the human cardiac fiber architecture from dt-mri. Proceedings of the 6th international conference on FIMH (2011) 171–179